The macrophage-stimulating protein pathway promotes metastasis in a mouse model for breast cancer and predicts poor prognosis in humans

Alana L. Welm*†, Julie B. Sneddon‡, Carmen Taylor§¶, Dimitry S. A. Nuyten‖, Marc J. van de Vijver‖, Bruce H. Hasegawa§¶, and J. Michael Bishop*

*The G. W. Hooper Foundation, and §Department of Radiology, Physics Research Laboratory, University of California, San Francisco, CA 94143; ‡Department of Biochemistry, Stanford University, Stanford, CA 94305; ¶Department of Bioengineering, University of California, Berkeley, CA 94704; and ‖Division of Diagnostic Oncology, Netherlands Cancer Institute, 1066 CX Amsterdam, The Netherlands

Contributed by J. Michael Bishop, March 16, 2007 (sent for review December 7, 2006)

A better understanding of tumor metastasis requires development of animal models that authentically reproduce the metastatic process. By modifying an existing mouse model of breast cancer, we discovered that macrophage-stimulating protein promoted breast tumor growth and metastasis to several organs. A special feature of our findings was the occurrence of osteolytic bone metastases, which are prominent in human breast cancer. To explore the clinical relevance of our model, we examined expression levels of three genes involved in activation of the MSP signaling pathway (*MSP*, *MT-SP1*, and *MST1R*) in human breast tumors. We found that overexpression of *MSP*, *MT-SP1*, and *MST1R* was a strong independent indicator of both metastasis and death in human breast cancer patients and significantly increased the accuracy of an existing gene expression signature for poor prognosis. These data suggest that signaling initiated by MSP is an important contributor to metastasis of breast cancer and introduce an independent biomarker for assessing the prognosis of humans with breast cancer.

bone metastasis | Ron | tumor | inflammation | prognostic factor

Breast cancer often results in metastasis to many organs, including lymph nodes, bone, lungs, brain, and liver. The most frequent site of breast cancer metastasis is the bone, which occurs in ≈80% of patients with advanced disease (1). To better understand metastasis of breast cancer, models are needed in which metastases spontaneously occur from tumors arising in the orthotopic site. Such models have been described, although they use immortalized cell lines and usually require immunodeficient hosts. We describe here the modification of a mouse model of breast cancer in which tumors originate from primary breast epithelial cells, and metastasis occurs from an orthotopic tumor in immunocompetent animals. This experimental system allows us to efficiently examine the effect of individual genes or combinations of genes on tumor behavior. In this study, we examined the role of macrophage-stimulating protein (MSP) in breast tumor growth and metastasis.

MSP was originally identified as a serum protein that elicited macrophage chemotaxis and activation (2, 3). MSP is secreted as an inactive single-chain precursor (pro-MSP), which becomes active after proteolytic cleavage to yield a disufide-linked heterodimer. The protease that activates pro-MSP was isolated from the extracellular membranes of macrophages (4) and has recently been identified as membrane-type serine protease-1 (MT-SP1, also known as matripase), which is expressed on macrophages and several types of epithelial cells, including breast cells (5).

The biological effects of MSP are not restricted to macrophages. In particular, MSP can promote migration of various epithelial cell lines (6, 7), and the receptor for MSP, macrophage-stimulating-1 receptor (MST1R, also known as Ron), can induce an epithelial-to-mesenchymal transition in immortalized canine kidney cells *in vitro* (8). Evidence is accumulating that the MSP/MST1R pathway is involved in cancer. For example, overexpression of MST1R caused transformation of cultured epithelial cell lines (9, 10) and led to tumor development in lungs of transgenic mice (11).

MT-SP1 and MST1R are overexpressed in ≈45% and 50% of human infiltrating breast carcinomas, respectively (12, 13). A recent study showed that overexpression of MST1R, together with its homolog Met, correlated with reduced disease-free survival of breast cancer patients (14). These data suggest that the MSP/MT-SP1/MST1R pathway may play a role in breast cancer. We used a mouse model of breast cancer to demonstrate that MSP facilitates tumor growth and metastasis, particularly to bones. We also found that concomitant expression of components of the MSP pathway represented a highly accurate independent prognostic indicator for metastasis and death and significantly increased the accuracy of an existing poor prognosis gene expression signature for breast cancer (15, 16).

Results

Development of a Versatile Orthotopic Mouse Model of Breast Tumorigenesis and Metastasis. To rigorously address the role of MSP in tumor progression and metastasis *in vivo*, we required a mouse model system in which metastasis might occur directly from the primary site, rather than as a result of cells having been injected into the bloodstream. We began with mammary tumors from transgenic mice that expressed the Polyomavirus Middle T antigen under control of the mouse mammary tumor virus promoter (17) (MMTV-PyMT). We chose the PyMT model, because detailed analysis has shown that PyMT tumors resemble human breast cancers. Specifically, PyMT tumors develop through a series of distinct histological stages that resemble progression of human breast cancer to malignancy (18). In addition, PyMT tumors display biomarkers that are relevant to progression of the human disease, such as loss of estrogen and progesterone receptors and overexpression of ErbB2/Neu and cyclin D1 (18). The PyMT oncogene also elicits a well characterized signaling cascade (19–21), leading

Author contributions: A.L.W. and J.M.B. designed research; A.L.W. and C.T. performed research; A.L.W., D.S.A.N., M.J.v.d.V., and B.H.H. contributed new reagents/analytic tools; A.L.W., J.B.S., C.T., D.S.A.N., B.H.H., and J.M.B. analyzed data; and A.L.W. and J.M.B. wrote the paper.

The authors declare no conflict of interest.

Freely available online through the PNAS open access option.

Abbreviations: MSP, macrophage-stimulating protein; MT-SP1, membrane-type serine protease 1; MST1R, macrophage-stimulating 1 receptor; PyMT, Polyomavirus middle T antigen; MMTV, mouse mammary tumor virus; CT, computed tomography; TRAP, tartrate-resistant acid phosphatase.

†To whom correspondence should be addressed at the present address: Department of Oncological Sciences, Huntsman Cancer Institute, University of Utah, 2000 Circle of Hope, Salt Lake City, UT 84112. E-mail: alana.welm@hci.utah.edu.

This article contains supporting information online at www.pnas.org/cgi/content/full/0702095104/DC1.

to activation of pathways known to be involved in human breast cancers (22).

Tumors initiated by overexpression of transgenic PyMT develop with 100% penetrance and relatively short latency. Whereas many existing transgenic mouse models of breast cancer do not exhibit metastasis, MMTV-PyMT tumors do metastasize, but only to the lungs (17). For our studies, tumors were harvested from either of two sources: MMTV-PyMT transgenic mice or mice bearing PyMT tumors resulting from transplantation of normal mammary epithelial cells that had been transduced *in vitro* (23) with the PyMT oncogene. To determine whether overexpression of MSP could promote tumor invasion and metastasis, we introduced MSP into tumors elicited by PyMT using either of two methods. In the case of MMTV-PyMT tumors, we introduced a replication-defective mouse stem cell virus (pMIG) that expressed MSP and GFP into primary mammary tumor cells. The tumor cells were infected with either the pMIG (GFP alone) retroviral vector or pMIG-MSP, and infected (GFP+) cells were sorted by flow cytometry and transplanted into cleared mammary fat pads of recipient mice. The transplants gave rise to tumors that expressed either GFP or MSP and GFP. In the case of PyMT tumors generated by retroviral transduction (pMIG-PyMT-IRES-GFP tumors), we introduced pMIG-MSP or pMIG into primary mammary tumor cells along with a retrovirus that contained a puromycin-resistance gene. The cells were selected for 2 days in puromycin before transplantation into cleared mammary fat pads. In both types of experiments, the transplanted tumor cells expressed the PyMT transgene and/or transduced genes, as expected. The results were similar using either method (data not shown), but we found generation of PyMT tumors by retroviral transduction to be advantageous, because the cell-sorting step was eliminated. Expression of GFP provided a reliable sensitive identifier of tumor cells that had metastasized to distant organs.

MSP Facilitated the Growth and Dissemination of Mammary Tumors in Mice. Tumors that expressed MSP (PyMT+MSP tumors) initially grew twice as fast as control tumors (PyMT+pMIG), although tumor growth reached a plateau, and the control tumors eventually achieved sizes comparable to PyMT+MSP tumors (Fig. 1*A*). Tumors that expressed MSP were more locally invasive than were control tumors [supporting information (SI) Fig. 4 *A* and *B*]. MSP was detected only in PyMT+MSP tumors (SI Fig. 4*C*). Both groups of tumors expressed MT-SP1 (SI Fig. 4*D*), but phosphorylated MSP receptor was detected only in tumors expressing MSP (SI Fig. 4*E*). Thus, overexpression of MSP in MMTV-PyMT tumors resulted in activation of the MSP receptor.

In our experiments, lung metastasis occurred at a frequency consistent with that previously reported for MMTV-PyMT mice (17) (see Table 1). Tumors that expressed MSP, however, metastasized earlier than control tumors (SI Fig. 5) and displayed a broadened spectrum of metastasis to a variety of other organs including lymph nodes, spleen, and bone (Table 1 and Fig. 1 *B–F*). Control tumors, even at the maximal tumor size, were never as metastatic as tumors expressing MSP, and never metastasized to bone (Table 1). Liver metastases were observed infrequently from both tumors expressing MSP and control tumors (Table 1). Brain metastases were not apparent, although brains were examined only in animals that displayed severe metastasis to other organs (data not shown).

MSP Promoted Osteolytic Bone Metastasis. A prominent effect of MSP expression in tumors was metastasis to bone, which occurred in ≈20% of the mice (Table 1). The most common site for bone metastasis was the distal femur, but metastases were also observed on the ribs, sternum, and tibia (data not shown). Computed tomography (CT) scans revealed loss of bone density due to osteolysis, which was apparent on CT cross-section images (Fig. 2*A*) and in 3D rendering of the CT data (Fig. 2*B*). Metastasis was confirmed after CT scanning by the presence of GFP-positive tumor cells (Fig. 2*C*). We observed GFP-positive tumor cells in the bone marrow both with fluorescent microscopy and by flow cytometry (data not shown), but tumors that expressed MSP were also able to invade through the leg muscle and directly into the bone (data not shown). Histologically, osteolysis was manifested by the appearance of pits in the bone matrix (Fig. 2*E*) and by the presence of tartrate-resistant acid phosphatase (TRAP)-positive osteoclasts at the site of resorption (Fig. 2*F*). Using an *in vitro* bone pit assay, we found that tumor cells that expressed MSP, but not control tumor cells, were able to stimulate activation of osteoclast-like cells, which resulted in erosion of bone matrix (Fig. 2 *H* and *I*). These data are consistent with our observation that bone osteolysis resulting from metastasis of tumors that expressed MSP was associated with an increase in osteoclasts at sites of bone metastases *in vivo*.

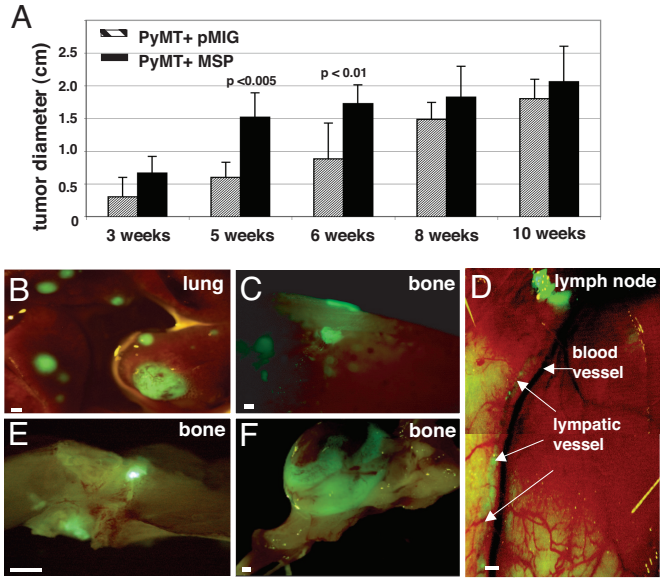

Fig. 1. Overexpression of MSP in tumors initiated by PyMT results in faster tumor growth and increased metastasis. (*A*) Diameter of PyMT+pMIG or PyMT+MSP tumors as a function of time after transplantation (measured upon necropsy). The data are represented as a mean ± standard deviation. (*B–F*) Fluorescent whole-mount images of PyMT+MSP metastases in lung, bone, and lymphatics. (*E* and *F*) Fluorescent whole-mount images of larger bone metastases in mice from which the primary tumors (PyMT+MSP) were surgically removed 6 months before analysis. (Scale bars: *A*, *B*, *D–F*, 1 mm; *C*, 100 μm.)

Coordinate Overexpression of *MSP*, *MT-SP1*, and *MST1R* Correlated with Metastasis and Death in Human Breast Cancer. To explore the relevance of our findings to human breast cancer, we examined

Table 1. MSP increases metastatic frequency of PyMT tumors to lung, lymph nodes, spleen, and bones

Site of metastasis	PyMT+pMIG, %	PyMT+MSP, %	*P* value*
Lung	42/82 (51)	68/99 (68)	<0.025
Lymph node	15/82 (18)	54/99 (54)	<0.001
Spleen	3/65 (4.6)	25/80 (31)	<0.001
Bone	0/75 (0)	20/95 (21)	<0.001
Liver	3/65 (4.6)	5/65 (7.6)	Not significant†

The frequency at which PyMT+pMIG or PyMT+MSP tumors metastasized to various organs is indicated by the fraction of mice that displayed GFP plus tumor cells in each organ, as determined by fluorescent whole-mount microscopy. The data represent a combination of all experiments, using MMTV-PyMT and pMIG-PyMT tumors as a source of transplanted cells.
*P values were determined by χ^2 analysis.

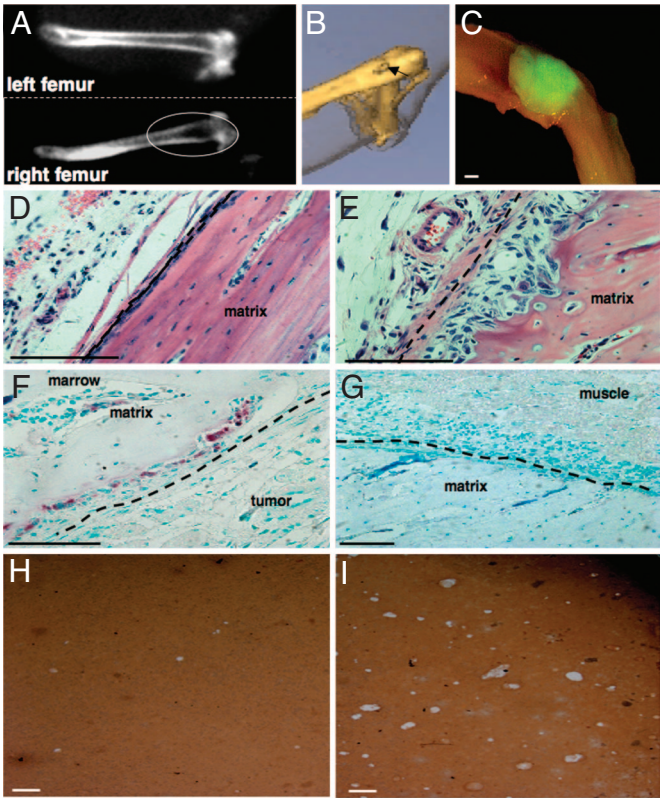

Fig. 2. Tumor cells overexpressing MSP metastasized to bone, resulting in osteolytic lesions. (*A*) CT cross-section images of the normal left femur and the affected right femur from a mouse bearing a PyMT+MSP tumor. The images were taken at the same time, and only the right femur was affected by metastasis. (*B*) 3D rendering of CT data from the same mouse as in *A*. The arrow shows loss of bone density in the femur just above the knee. (*C*) Fluorescent whole-mount microscopy of the femur after the CT scan, showing a GFP+ PyMT+MSP tumor near the right knee. (*D*) Hematoxylin/eosin stain of a section of a normal femur. (*E*) Hematoxylin/eosin stain of a femur near a metastatic tumor, showing pitting of the bone beneath the periosteum (dashed line). (*F*) TRAP stain of the bone, showing osteoclasts in the bone pits (purple stain). The periosteum is indicated by the dashed line. (*G*) TRAP stain of the same bone in the region distal to the tumor. (Scale bar: *C*, 1 mm; *D–G*, 100 μm.) (*H* and *I*) *In vitro* bone pit assays using osteoclast-like cells derived from mouse bone marrow and cocultured with PyMT+pMIG primary tumor cells (*H*) or PyMT+MSP bone metastasis tumor cells (*I*). The bone matrix stains brown, and the pits induced by osteoclasts appear as white patches. (Scale bars, 100 μm.)

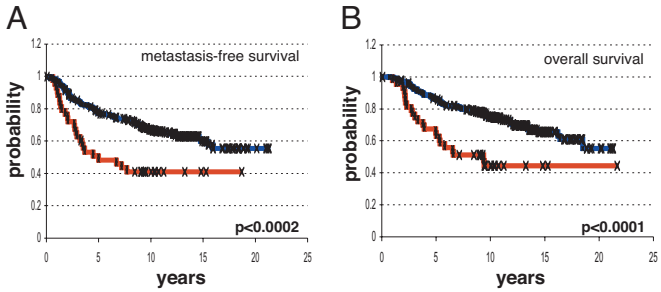

Fig. 3. Overexpression of the *MSP/MST1R* pathway in human breast cancer is associated with metastasis and death. (*A*) Kaplan–Meier analysis showing development of metastases over time for two groups of patients: those whose tumors expressed *MSP/MST1R/MT-SP1* (according to *MSP* oligonucleotide 2) at levels above the mean (red line), and those whose tumors did not express all three genes above the mean (blue line). (*B*) Kaplan–Meier analysis showing time to death for the same groups of patients as in *A*. *P* values were calculated by using the log-rank test.

microarray gene expression data from 295 breast cancer patients from the Netherlands Cancer Institute studies (16). We found that *MSP* gene expression alone was not prognostic for outcome in human breast cancer (data not shown); however, because the biological effects of MSP depend on its proteolytic activation and the ability to bind to its receptor (2), expression of all three genes (*MSP*, *MT-SP1*, and *MST1R*) would be required for activation of the MSP pathway. Thus, we determined whether *MSP*, *MT-SP1*, and *MST1R* were overexpressed coordinately in breast cancer.

The arrays contained one oligonucleotide each corresponding to *MT-SP1* and *MST1R* but happened to contain two different oligonucleotides corresponding to *MSP*. Some patients appeared to express *MSP* differently according to the two *MSP* oligonucleotides. This was purely an empirical observation, although there are two different *MSP* transcripts (24), which have different affinities for the two *MSP* oligonucleotides (data not shown). Faced with uncertainties about which *MSP* oligonucleotide might provide the more decisive conclusion, we analyzed the results with all four possible permutations: using oligonucleotide 1 only, using oligonucleotide 2 only, combining results obtained with each oligonucleotide (identifying patients positive for either oligonucleotide), and using both oligonucleotides (identifying patients positive for both oligonucleotides). Every permutation revealed significant prognostic value when the three components of the MSP signaling pathway were expressed concomitantly, although the strength and scope of the prognoses varied. In the presentation that follows, we use the results with oligonucleotide 2 for illustrative purposes, with secondary reference to the other permutations presented in *SI Text*.

Using MSP oligonucleotide 2, we found that 43/295 (14.6%) of primary breast tumors in the Netherlands Cancer Institute (NKI) data set coordinately expressed *MSP*, *MT-SP1*, and *MST1R* at above-average levels. The number of patients defined as overexpressing *MSP*, *MT-SP1*, and *MST1R* ranged from 7.5% to 19.6%, depending on the *MSP* oligonucleotide used (SI Table 4). Kaplan–Meier analysis showed that patients whose tumors overexpressed *MSP/MT-SP1/MST1R* had significantly shorter metastasis-free survival ($P = 0.0002$, Fig. 3*A*) and overall survival ($P = 0.0001$, Fig. 3*B*) compared with patients whose tumors did not overexpress all three genes. The correlation with poor outcome was significant, no matter which MSP oligonucleotide(s) was used (SI Fig. 6). Patients whose tumors coordinately expressed *MSP/MST1R/MT-SP1* below the mean did not benefit from significantly longer metastasis-free survival or overall survival, and overexpression of *MSP*, *MT-SP1*, or *MST1R* alone, or any combination of two of these three genes, did not reveal any significant association with clinical outcome in this data set (data not shown).

Because overexpression of *MSP/MT-SP1/MST1R* significantly correlated with overall metastasis (Fig. 3*A*), we investigated whether overexpression of these genes correlated with metastasis to specific organs. We found that patients with tumors that overexpressed *MSP/MT-SP1/MST1R* experienced a significantly increased incidence of metastasis to bone ($P < 0.025$), lung ($P < 0.001$), liver ($P < 0.05$), and brain ($P < 0.05$). Bone was the most common site of metastasis for all patients (Table 2).

Overexpression of *MSP*, *MT-SP1*, and *MST1R* Was an Independent Prognostic Factor for Metastasis and Death in Human Breast Cancer Patients. We analyzed potential associations of *MSP/MST1R/MT-SP1* overexpression with other clinical parameters, including patient age, number of positive lymph nodes, tumor size, histological grade, and estrogen receptor status. We found no statistically significant association with factors other than metastasis and death (data not shown). We also found no significant association between *MSP/MST1R/MT-SP1* overexpression and previously described gene expression signatures (15, 16, 25, 26). To more rigorously address the independence of *MSP/MST1R/MT-SP1* overexpression

Table 2. Percentage of patients that experienced metastasis to various sites

Site of metastasis	*MSP/MT-SPT/MST1R*+ tumors (n = 13), %	Other tumors (n = 252), %	P value
Bone	44.2	27.4	<0.025
Lung	25.6	6.7	<0.001
Brain	14.0	4.8	<0.05
Liver	27.9	15.9	<0.05
Lymph	11.6	4.8	<0.1
Meninges	7.0	1.6	<0.1
Pleura	14.0	7.9	0.2
Skin	7.0	2.4	1
Any lymph node	14.0	8.3	1
Peritoneum	4.7	2.8	1

The patients are arranged in two groups: those whose tumors overexpressed *MSP/MST1R/MT-SP1* (according to *MSP* oligonucleotide 2), and the rest of the patients. P values were determined by using the χ^2 test.

in prognosticating patient outcome, we carried out multivariate proportional-hazards analysis (27) using distant metastasis as the first event and overall survival as endpoints. We used multivariate analysis to compare the prognostic value of our results to the value of parameters currently used in the clinic and of recently identified gene expression signatures (15, 16, 25, 26). We found that coordinate overexpression of *MSP/MST1R/MT-SP1* was an independent prognostic factor for risk of both metastasis and death, with a hazard ratio of 2.87 and 3.22, respectively ($P \leq 0.001$; Table 3 and SI Table 5). The only other independent prognostic factors for survival in this analysis were tumor diameter ($P = 0.05$) and a "poor-prognosis" gene expression signature ($P \leq 0.001$), which consists of 70 genes whose coordinate expression is strongly prognostic for a short interval to metastasis (15). The signature was identified by supervised classification, trained on a subset of the patient samples included in our analysis (15, 16). Overexpression of *MSP/MST1R/MT-SP1* was a strong independent prognostic factor for risk of both metastasis and death, no matter which *MSP* oligonucleotide(s) was used (SI Table 4).

Assessment of *MSP/MST1R/MT-SP1* Expression Improved the Prognostic Accuracy of the 70-Gene Poor Prognosis Signature. *MSP*, *MT-SP1*, and *MST1R* are not members of the 70-gene prognostic signature (15), yet we found that coordinate overexpression of these three genes was a strong independent prognostic factor for poor outcome. Despite its high specificity, however, coordinate overexpression of *MSP/MT-SP1/MST1R* as a single prognostic factor was not sensitive enough to identify all patients that experienced metastasis. This prompted us to investigate whether predictions based on overexpression of *MSP/MT-SP1/MST1R* could provide additional prognostic benefit when used together with the 70-gene signature.

Using *MSP* oligonucleotide 2, we found that detection of *MSP/MT-SP1/MST1R* overexpression in tumors can improve the accuracy of prognoses for poor outcome made by the 70-gene "poor prognosis" signature. The 70-gene signature predicted that 61% of the 295 patients would have a poor outcome, but only half of these patients actually developed metastases or died by 2005 (51% accuracy over a 10-year minimum followup time). We found that 27/295 patients (9.1%) displayed both the 70-gene "poor prognosis" signature and overexpression of *MSP/MT-SP1/MST1R*. Over the same 10-year minimum followup period, 82% of these patients developed metastasis or died. Therefore, a combination of the 70-gene "poor prognosis" signature and overexpression of *MSP*, *MT-SP1*, and *MST1R* provided a significant improvement in prognostic accuracy over the 70-gene "poor prognosis" signature alone ($P < 0.01$), and this applied to 9.1% of breast cancer patients in this study. Overexpression of *MSP/MST1R/MT-SP1* always significantly improved the accuracy of the 70-gene "poor prognosis" signature, no matter which *MSP* oligonucleotide(s) was used (SI Table 6). The number of breast cancer patients in this study that displayed both the 70-gene "poor prognosis" signature and overexpression of *MSP/MT-SP1/MST1R*, and would thus benefit from the improved accuracy of the prognosis, ranged from 4% to 12%, depending on which *MSP* oligonucleotide(s) was used (SI Table 6).

***MSP/MT-SP1/MST1R* Was Validated as a Marker of Poor Prognosis in an Independent Set of Patients.** To validate our finding that *MSP/MT-SP1/MST1R* was a prognostic factor for poor outcome in breast cancer, we analyzed data from an independent study. The second data set comprised microarray gene expression data from 162 primary tumors collected from a diverse cohort of patients from four institutions (28, 29). We refer to this collection as the University of North Carolina Utah (UNC/Utah)/Utah data set. Patients in the UNC/Utah collection differed from the NKI cohort with respect to both age and stage of disease and are likely more representative of all women with breast cancer (see *SI Text*).

We found that 10/162 (6.2%) of primary breast tumors in the UNC/Utah collection coordinately expressed *MSP*, *MT-SP1*, and *MST1R* at above-average levels. Kaplan–Meier analysis showed that patients whose tumors overexpressed *MSP/MT-SP1/MST1R* had significantly shorter relapse-free survival ($P = 0.03$; SI Fig. 7) compared with the rest of the patients. We did not see a significant association with *MSP/MT-SP1/MST1R* status and overall survival to date (data not shown), although the patients in the UNC/Utah collection have been followed for a much shorter time than those in the NKI collection (median time, 21.5 months vs. 10.2 years).

We also investigated whether *MSP/MT-SP1/MST1R* status could improve the accuracy of the 70-gene "poor" prognosis in the UNC/Utah dataset. We found that, in these patients to date, the

Table 3. Multivariate Cox proportional-hazards analysis of the risk of death in breast cancer patients

Variable (endpoint: survival)	Hazard ratio (95% CI)*	P value
MSP/MT-SP1/MST1R expression (above mean vs. below mean)	3.22 (1.98–5.26)	<0.001
Poor-prognosis signature (vs. good-prognosis signature)	3.49 (1.74–7.00)	<0.001
Tumor diameter (>2 vs. <2 cm)	1.55 (1.00–2.37)	0.05
Patient age (>40 vs. <40 years)	0.69 (0.44–1.07)	0.1
Wound signature (positive vs. negative)	1.41 (0.86–2.33)	0.18
Sorlie subtype (basal or luminal B vs. normal or luminal A)	1.39 (0.76–2.54)	0.29
Tumor grade (grade III vs. grades I or II)	1.10 (0.67–1.79)	0.71
Estrogen receptor expression (positive vs. negative)	0.95 (0.59–1.54)	0.84
Lymph node status (positive vs. negative)	1.00 (0.66–1.53)	1

Cox proportional-hazards analysis was carried out by using binary variables as indicated. Analysis was carried out by defining MSP expression according to oligonucleotide 2.
*The numbers in parentheses indicate the range at the 95% confidence interval (CI).

accuracy of the 70-gene "poor prognosis" signature was 28%. When *MSP*/*MT-SP1*/*MST1R* expression and the 70-gene "poor prognosis" signature were combined, the accuracy was 56% ($P = 0.1$). Although not statistically significant, these data show a trend toward improvement of accuracy of the 70-gene "poor prognosis" signature in the UNC/Utah patients. Significance will likely be improved upon analysis of more patients and/or a longer clinical followup time.

Discussion

We have used a mouse model of breast cancer to demonstrate that *MSP* promotes tumor growth and metastasis, including osteolytic metastasis to bone, from the site of the primary tumor. These findings provide the first indication that *MSP* facilitates metastasis. Our results complement a recent finding that targeted deletion of the MST1R kinase domain in the MMTV-PyMT model of breast cancer caused a reduction in tumor growth and metastasis to lungs (30). The MST1R study, however, could not investigate a role for the MSP pathway in metastasis to other organs, because the mice used in that study do not exhibit metastasis to sites other than lung (17, 30).

Although primary tumors expressing MSP grew faster than control tumors, we did not detect an increase in the number of cycling cells or a decrease in apoptotic cells (data not shown), suggesting that MSP does not promote metastasis simply by promoting tumor cell survival or proliferation. Also, the increased incidence of metastasis does not appear to be secondary to a rise in tumor cell numbers: transplantation of 10-fold more control tumor cells than MSP-expressing tumor cells caused the control tumors to grow faster but did not recapitulate the pattern or frequency of metastasis seen in tumors expressing MSP (A.L.W. and J.M.B., unpublished data). MSP may instead promote metastasis by affecting the ability of tumor cells to migrate, invade the extracellular matrix and blood vessels, and/or grow in distant tissues. The direct activation of osteoclasts by tumor cells expressing MSP suggests a mechanism by which MSP could facilitate growth in the bone.

Macrophage infiltration is a feature of invasive cancers and is associated with poor prognosis in breast cancer (31, 32). Macrophages are important for lung metastasis in the MMTV-PyMT mice from which we obtained the tumors used in our studies (33). Because MSP activates macrophages, it is possible that the effects of MSP occur through a mechanism involving inflammation. Our *in vitro* data showed that recombinant MSP was sufficient to stimulate mammary epithelial cells to invade extracellular matrix, indicating that these cells can directly respond to MSP. The effect of MSP was augmented, however, when macrophages were cocultured with the epithelial cells (A.L.W. and J.M.B., unpublished data). We also attempted to address the requirement for macrophages in our model system *in vivo* using *csf1*-deficient (*op*/*op*) mice (34), but we found large variations in tumor growth and metastasis in the *op*/*op* background that made our results impossible to interpret. Therefore, it is still unknown whether macrophages play a role in MSP-induced metastasis *in vivo*.

The replication of clinically relevant metastasis in our mouse model prompted us to investigate *MSP* gene expression in human breast cancer. Analysis of a total of 457 breast tumors from two independent studies showed a significant correlation between *MSP*/*MT-SP1*/*MST1R* overexpression and poor outcome. Approximately two-thirds of patients whose tumors overexpressed *MSP*/*MT-SP1*/*MST1R* had poor outcome: they experienced increased metastasis to bone, lung, liver and brain and had shorter survival times. It should be noted, however, that whereas nearly 80% of women with breast cancer experience bone metastasis, a much smaller fraction of breast cancers overexpressed *MSP*/*MT-SP1*/*MST1R* in our analyses (up to 19.6% in the NKI data set and 6.2% in the UNC/Utah set). These data suggest that pathways other than the MSP pathway may contribute to bone metastasis.

Analysis of expression of *MSP*/*MT-SP1*/*MST1R* in concert with the previously described 70-gene "poor prognosis" signature significantly increased the accuracy with which poor outcome was prognosticated for breast cancer patients. These data suggest that a greater prognostic power would result from addition of *MSP*, *MT-SP1*, and *MST1R* oligos to the existing 70-gene array, so that *MSP*/*MT-SP1*/*MST1R* expression status can be considered in parallel with the prognosis signature. Even the least stringent analysis of the NKI data (which defined patients according to a positive signal from either MSP oligonucleotide) significantly increased the accuracy of the 70-gene signature for 12% of patients, which would currently represent >25,000 people per year based on an annual diagnosis rate of >212,000 (see www.komen.org).

The gene expression data used in the first part of this study were gathered from 295 tumors collected from patients with stage I or II breast cancer (16). Our data indicate that coordinate overexpression of *MSP*, *MT-SP1*, and *MST1R* is a prognostic factor for poor outcome in early stage disease, which may aid in treatment decisions. We also validated our findings on an independent collection of 162 breast tumors from individuals with a wider range of disease stages, albeit with shorter followup to date.

Together, our findings implicate MSP as an important contributor to metastasis and highlight how the study of mouse models can inform the analysis of clinical data. Our model should be useful for preclinical studies to determine whether disruption of the MSP pathway is effective in slowing tumor growth and reducing or preventing metastasis.

Experimental Procedures

Animals. Animals were handled according to protocols approved by the University of California, San Francisco, Institutional Animal Care and Use Committee. MMTV-PyMT mice were obtained from The Jackson Laboratory, (Bar Harbor, ME). Some mice underwent a second surgery to remove the primary tumor, which was 2–2.5 cm in diameter at the time of resection.

Infection of Cells with Retroviruses. Retroviral production and infections were as described (23). Infection of MMTV-PyMT tumor cells was carried out as for normal mammary epithelial cells except that, after collagenase treatment, the tumors were plated on 150-mm tissue culture dishes overnight, then trypsinized and plated at a density of 10^5 cells/well in six-well dishes for infection the next day. Infected MMTV-PyMT tumor cells were sorted for GFP by using a FACSVantage SE cell sorter, and the cells were transplanted immediately. To generate tumors expressing PyMT by retroviral transduction, normal mammary epithelial cells were infected with pMIG-PyMT. The cells were transplanted into cleared mammary fat pads (10^6 cells/gland), and tumors developed in ≈3 months. pMIG-PyMT tumor cells were isolated and infected with pMIG-MSP or pMIG, plus a retrovirus containing a puromycin resistance gene at a ratio of 2:1. Puromycin was added at a concentration of 1 μg/ml beginning 1 day after infection. Selection continued until transplantation (4 days after tumor harvest).

CT. microCT was performed on a combined microSPECT/microCT scanner for small animals (X-SPECT; Gamma Medica Ideas, Northridge, CA). Mice were anesthetized with isoflurane during image acquisition. Tomographic data were acquired at 512 angles over 360° at 50 kilovoltage peak tube potential and 600 μA tube current. Images were reconstructed with the Feldkamp cone-beam algorithm (Gamma Medica Ideas) and imported into Amira (Mercury Computing Systems, Chelmsford, MA) for processing and analysis. Transaxial images were oriented to obtain cross-sectional views through individual vertebrae and along the axes of both femurs. The entire skeleton was surface-rendered as a 3D volumetric image as an aid to visualization.

Osteoclast Assays. TRAP staining was performed as described (35). For *in vitro* assays, osteoclast-like cells were prepared from mouse bone marrow as described (36). The cells were plated on osteologic discs (BD Biosciences, San Jose, CA) for bone pit assays. After 5 days, PyMT+pMIG or PyMT+MSP tumor cells were added to the osteoclast cultures at a density of 10^5 tumor cells per well. Five days later, the cells were removed with bleach, and the discs were stained according to the manufacturer.

Gene Expression Analysis. Gene expression data for *MSP1*, *MT-SP1*, and *MST1R* were culled for each tumor sample from the NKI data set by mapping Unigene identifiers from build 158, release date January 18, 2003. Two clones were mapped for *MSP1*, corresponding to Unigene ID 349110. One clone each was mapped for *MT-SP1* (Unigene ID 56937) and *MST1R* (Unigene ID 2942). Gene expression data for all four clones were extracted for each sample and mean-centered across all samples for each clone. Samples were segregated into groups for each analysis. Group A comprised tumors coordinately expressing *MT-SP1*, *MST1R*, and *MSP* (according to oligonucleotide 2) at levels higher than the mean (43 tumors), and group B comprised the remaining samples (252 tumors). Detailed information on analysis of the different *MSP*/*MT-SP1*/*MST1R* groups using all possible permutations can be found in *SI Text*. Information on metastasis and survival was obtained by using followup data as of January 1, 2005, which represents an update of the 2001 data published previously (16). The same method was used for the UNC/Utah data set (see *SI Text* for more information).

Statistical Analysis. Kaplan–Meier survival curves were generated by using the software package WINSTAT FOR EXCEL (R. Fitch Software, Staufen, Germany). Multivariate analysis was performed by using the Cox proportional-hazard method and SPSS 13 software (SPSS, Chicago, IL). Covariates analyzed in the multivariate analysis included the following binary variables: tumor diameter (up to and including 2 vs. >2 cm), positive lymph nodes (zero vs. one or more positive nodes), tumor grade (I or II vs. III), patient age (≤40 vs. >40 year), estrogen receptor status (negative vs. positive), wound signature ("quiescent" vs. "activated"), poor prognosis signature ("good" vs. "poor"), Sorlie subtype (normal-like or luminal A vs. luminal B, basal, or ErbB2-like), and MSP pathway status (group B vs. A). For each sample, assignment according to the wound signature as "quiescent" or "activated" was made on the basis of unsupervised clustering of the entire NKI data set with the wound signature genes, as reported (25, 37). Assignment to the five-class "intrinsic gene signature" or Sorlie subtype was made by matching the expression of the intrinsic genes in each tumor sample to the most similar expression centroid for the five classes, as described (25, 26, 38). Classification of good or poor prognosis according to the Poor Prognosis Signature has been described (15, 16).

Note Added in Proof. Overexpression of murine Ron was recently shown to induce mammary tumor formation and metastasis to lung and liver (39), providing further evidence of the importance of the MSP pathway in breast cancer.

We thank Luda Urisman for technical assistance, as well as members of the Bishop laboratory for helpful discussions. We thank William Muller (McGill University) for making the MMTV-PyMT transgenic mice available and Yosef Refaeli (National Jewish Medical Research Center, Denver, CO) for providing the pMIG vector. We are grateful to Kirk Jones for consultation with histology, Thomas Link for assistance in reading CT scans, Patrick Brown for assistance in interpreting microarray data, Philip Bernard and Charles Perou for access to the UNC/Utah data set, and Ami Bhatt and Charles Craik for access to data before publication and discussions about MT-SP1. This work was supported by the G. W. Hooper Research Foundation, National Institutes of Health Grant CA44338 (to J.M.B.), University of California Discovery Grant bio02-10300 with Gamma Medica IDEAS, Inc., as a private sponsor (to B.H.H.), and National Institutes of Health Bioengineering Research Partnership Grant 5 R01 EB000348 (to B.H.H.). A.L.W. was supported by Susan G. Komen Breast Cancer Foundation Grant PDF0201190. J.B.S. is supported by a predoctoral fellowship from the National Science Foundation. C.T. is supported by a predoctoral bioengineering fellowship from the Whitaker Foundation. D.S.A.N and M.J.d.V are supported by Dutch Cancer Society Grant NKB 2002-2575.

1. Jemal A, Tiwari RC, Murray T, Ghafoor A, Samuels A, Ward E, Feuer EJ, Thun MJ (2004) *CA Cancer J Clin* 54:8–29.
2. Leonard EJ (1997) *Ciba Found Symp* 212:183–191; discussion 192–187.
3. Lutz MA, Correll PH (2003) *J Leukocyte Biol* 73:802–814.
4. Wang MH, Skeel A, Leonard EJ (1996) *J Clin Invest* 97:720–727.
5. Bhatt AS, Welm AL, Farady CJ, Vasquez M, Wilson K, Craik C (2007) *Proc Natl Acad Sci USA* 104:5771–5776.
6. Santoro MM, Gaudino G, Marchisio PC (2003) *Dev Cell* 5:257–271.
7. Wang MH, Montero-Julian FA, Dauny I, Leonard EJ (1996) *Oncogene* 13:2167–2175.
8. Wang D, Shen Q, Chen YQ, Wang MH (2004) *Oncogene* 23:1668–1680.
9. Peace BE, Hughes MJ, Degen SJ, Waltz SE (2001) *Oncogene* 20:6142–6151.
10. Wang MH, Wang D, Chen YQ (2003) *Carcinogenesis* 24:1291–1300.
11. Chen YQ, Zhou YQ, Fisher JH, Wang MH (2002) *Oncogene* 21:6382–6386.
12. Kang JY, Dolled-Filhart M, Ocal IT, Singh B, Lin CY, Dickson RB, Rimm DL, Camp RL (2003) *Cancer Res* 63:1101–1105.
13. Maggiora P, Marchio S, Stella MC, Giai M, Belfiore A, De Bortoli M, Di Renzo MF, Costantino A, Sismondi P, Comoglio PM (1998) *Oncogene* 16:2927–2933.
14. Lee WY, Chen HH, Chow NH, Su WC, Lin PW, Guo HR (2005) *Clin Cancer Res* 11:2222–2228.
15. van 't Veer LJ, Dai H, van de Vijver MJ, He YD, Hart AA, Mao M, Peterse HL, van der Kooy K, Marton MJ, Witteveen AT, *et al.* (2002) *Nature* 415:530–536.
16. van de Vijver MJ, He YD, van't Veer LJ, Dai H, Hart AA, Voskuil DW, Schreiber GJ, Peterse JL, Roberts C, Marton MJ, *et al.* (2002) *N Engl J Med* 347:1999–2009.
17. Guy CT, Cardiff RD, Muller WJ (1992) *Mol Cell Biol* 12:954–961.
18. Lin EY, Jones JG, Li P, Zhu L, Whitney KD, Muller WJ, Pollard JW (2003) *Am J Pathol* 163:2113–2126.
19. Guy CT, Muthuswamy SK, Cardiff RD, Soriano P, Muller WJ (1994) *Genes Dev* 8:23–32.
20. Rauh MJ, Blackmore V, Andrechek ER, Tortorice CG, Daly R, Lai VK, Pawson T, Cardiff RD, Siegel PM, Muller WJ (1999) *Mol Cell Biol* 19:8169–8179.
21. Webster MA, Hutchinson JN, Rauh MJ, Muthuswamy SK, Anton M, Tortorice CG, Cardiff RD, Graham FL, Hassell JA, Muller WJ (1998) *Mol Cell Biol* 18:2344–2359.
22. Bieche I, Onody P, Tozlu S, Driouch K, Vidaud M, Lidereau R (2003) *Int J Cancer* 106:758–765.
23. Welm AL, Kim S, Welm BE, Bishop JM (2005) *Proc Natl Acad Sci USA* 102:4324–4329.
24. Degen SJ, McDowell SA, Waltz SE, Gould F, Stuart LA, Carritt B (1998) *DNA Seq* 8:409–413.
25. Chang HY, Nuyten DS, Sneddon JB, Hastie T, Tibshirani R, Sorlie T, Dai H, He YD, van't Veer LJ, Bartelink H, *et al.* (2005) *Proc Natl Acad Sci USA* 102:3738–3743.
26. Sorlie T, Perou CM, Tibshirani R, Aas T, Geisler S, Johnsen H, Hastie T, Eisen MB, van de Rijn M, Jeffrey SS, *et al.* (2001) *Proc Natl Acad Sci USA* 98:10869–10874.
27. Cox D (1972) *J R Stat Soc B* 34:187–220.
28. Hu Z, Fan C, Oh DS, Marron JS, He X, Qaqish BF, Livasy C, Carey LA, Reynolds E, Dressler L, *et al.* (2006) *BMC Genomics* 7:96.
29. Perreard L, Fan C, Quackenbush JF, Mullins M, Gauthier NP, Nelson E, Mone M, Hansen H, Buys SS, Rasmussen K, *et al.* (2006) *Breast Cancer Res* 8:R23.
30. Peace BE, Toney-Earley K, Collins MH, Waltz SE (2005) *Cancer Res* 65:1285–1293.
31. Lin EY, Pollard JW (2004) *Novartis Found Symp* 256:158–168; discussion 168–172:259–269.
32. Lin EY, Pollard JW (2004) *Br J Cancer* 90:2053–2058.
33. Lin EY, Nguyen AV, Russell RG, Pollard JW (2001) *J Exp Med* 193:727–740.
34. Yoshida H, Hayashi S, Kunisada T, Ogawa M, Nishikawa S, Okamura H, Sudo T, Shultz LD (1990) *Nature* 345:442–444.
35. Ortega N, Behonick DJ, Colnot C, Cooper DN, Werb Z (2005) *Mol Biol Cell* 16:3028–3039.
36. Kurihara N, Iwama A, Tatsumi J, Ikeda K, Suda T (1996) *Blood* 87:3704–3710.
37. Chang HY, Sneddon JB, Alizadeh AA, Sood R, West RB, Montgomery K, Chi JT, van de Rijn M, Botstein D, Brown PO (2004) *PLoS Biol* 2:E7.
38. Sorlie T, Tibshirani R, Parker J, Hastie T, Marron JS, Nobel A, Deng S, Johnsen H, Pesich R, Geisler S, *et al.* (2003) *Proc Natl Acad Sci USA* 100:8418–8423.
39. Zinser GM, Leonis MA, Toney K, Pathrose P, Thobe M, Kader SA, Peace BE, Beauman SR, Colllins MH, Waltz SE (2006) *Cancer Res* 66:11967–11974.